Edge Fluctuations and Global Confinement with Lower Hybrid Current Drive in the ASDEX Tokamak

J. Stöckel, F.X. Söldner, L. Giannone, F. Leuterer, K.-H. Steuer
and ASDEX team

IPP 1/268

March 1992

MAX-PLANCK-INSTITUT FÜR PLASMAPHYSIK

8046 GARCHING BEI MÜNCHEN

MAX-PLANCK-INSTITUT FÜR PLASMAPHYSIK

GARCHING BEI MÜNCHEN

Edge Fluctuations and Global Confinement with Lower Hybrid Current Drive in the ASDEX Tokamak

J. Stöckel, F.X. Söldner, L. Giannone, F. Leuterer, K.-H. Steuer
and ASDEX team

IPP 1/268 March 1992

Die nachstehende Arbeit wurde im Rahmen des Vertrages zwischen dem Max-Planck-Institut für Plasmaphysik und der Europäischen Atomgemeinschaft über die Zusammenarbeit auf dem Gebiete der Plasmaphysik durchgeführt.

Edge Fluctuations and Global Confinement with Lower Hybrid Current Drive in the ASDEX Tokamak*

J. Stöckel†, F.X. Söldner, L. Giannone, F. Leuterer, K.-H. Steuer and ASDEX team

Max-Planck-Institut für Plasmaphysik
EURATOM-IPP Association
8046 Garching bei München
Germany

Abstract

Electrostatic edge fluctuations were investigated by means of Langmuir probes on the ASDEX tokamak in lower hybrid current drive regimes, simultaneously with the global particle and energy balances.

It was found that the edge fluctuations are reduced and the global particle/energy confinement improves when the LH power is below the initial ohmic power. The maximum reduction of the fluctuations and the best confinement occur when the total power input (OH + LH) is minimum. With a LH power higher than the initial OH value, the fluctuation level increases noticeably, while no improvement of the global confinement is observed. The increase of the edge fluctuations seems to be poloidally localized and caused by local power deposition in front of the grill antenna. Therefore, the relative positions of the probe and antenna structure have to be taken into account for correct interpretation of the fluctuation data.

*This report is an expanded version of material which was originally a contributed presentation at the 18th EPS Plasma Physics Division Conference, Berlin, Germany, June 1991

†Permanent address: Institute of Plasma Physics, Czech. Acad. Sci., Za Slovankou 3, P.O.Box 17, 182 11, Praha 8, Czechoslovakia

1 Introduction

The confinement capability of the tokamak plasma with lower hybrid current drive (LHCD) is of crucial importance for efficient future applications.

Up to now, it is only *the global energy balance* that has been extensively investigated. In general, a deterioration of the global energy confinement with power is observed for LHCD similarly to other additional heating methods. This has been demonstrated on, for example, ASDEX [1] in the 2.45 GHz experiment . There, the global confinement time τ_E degrades with the total power P_{TOT}, the dependence of τ_E on P_{TOT} being well fitted by Goldstone scaling. On the other hand, at low densities ($\bar{n}_e \doteq 1.3{\cdot}10^{19}\ m^{-3}$) and relatively low LH powers ($P_{LH} \leq P^o_{OH}$), the energy content noticeably exceeds the corresponding OH value, while the total power input remains close to the initial P^o_{OH}. It is therefore deduced that the global energy confinement is improved in this particular case. Similar behaviour is also reported from, for example, the ALCATOR-C [2], PLT [3] and PETULA B [4] tokamaks. The improvement of τ_E under these conditions is generally interpreted as a direct consequence of the superior energy confinement of suprathermal electrons created by the LH wave.

The particle confinement with LHCD has not been studied quite as systematically. Nevertheless, an increase of the global particle confinement time τ_p has been observed on T-7 [5] and VERSATOR [6] (by a factor of 2) and WT-3 [7] (by a factor of about 1.5) tokamaks at $P_{LH} \leq P^o_{OH}$ and low densities as well, but no reasonable explanation has been proposed.

The improved particle confinement could possibly be explained in terms of the edge electrostatic fluctuations, which are generally assumed to be responsible for global particle losses, at least in OH tokamaks (see, for example, TEXT results [8]). Such an idea was recently supported by experiments on the CASTOR tokamak [9,10,11], where simultaneous reduction of the edge fluctuations and improvement of the global particle confinement during LHCD shots was observed. A reduction of the electrostatic fluctuations was also measured on DITE [12] under similar conditions.

The aim of this report is to investigate simultaneously the level of edge electrostatic fluctuations and the global particle/energy confinement for a well-defined, low-density LHCD regime on ASDEX. Attention is focused on the variation of these quantities with LH power (starting with $P_{LH} \ll P^o_{OH}$) to study the transition from improved to deteriorated confinement in more detail.

First we describe the experimental arrangement and details of measurement of the edge electrostatic fluctuations by Langmuir probes. In Section 3, the LHCD regime is documented and the behaviour of the global energy/particle confinement during the LH power scan is demonstrated. Evolution of the edge fluctuations under the same discharge conditions is discussed in Section 4. Finally, the results are summarized in the last section.

2 Experimental arrangement

The LHCD experiment was performed on the ASDEX tokamak at the frequency f = 2.45 GHz. The LH antenna structure consists of two independently powered parts, denoted as the upper and lower grills. Phasing of the waveguide array was $\phi = 90^o$, and the resulting power spectrum is centred around $N_{||} = c/v_{||} = +2.2$ [13]. The major radius and radius of the outer separatrix were kept at $R = 168$ cm and $R_s = 208$ cm, respectively. The position of the LH antenna was fixed at $R_g = 212.5$ cm.

A multiple-tip Langmuir probe for fluctuation measurements is located near the equatorial plane ($R_{probe} = 211$ cm), 21^o in the toroidal direction away from the LH antenna. Since it was found that the relative positions of the probe and LH antenna structure play an important role in interpreting the probe data, they are discussed in detail in Sec. 4.

The experimental set-up of the fluctuation measurements is shown in Fig. 1. We used here three poloidally separated tips, assumed to be on the same magnetic

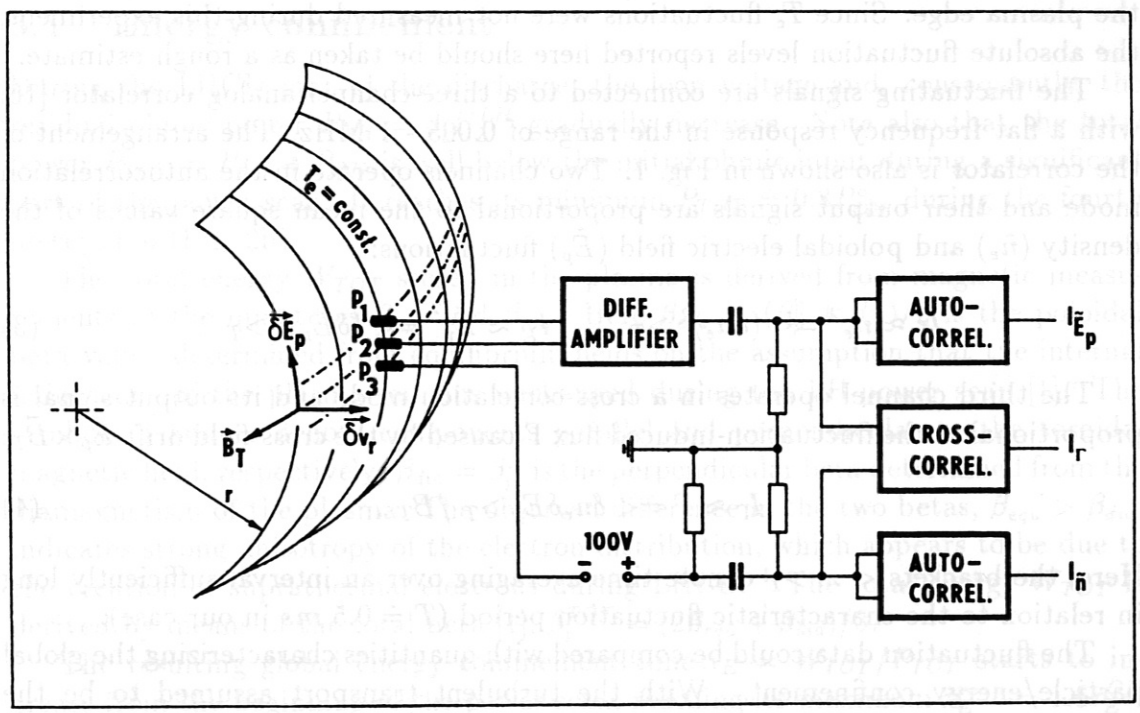

Figure 1: Schematic arrangement of the Langmuir probe tips and a three-channel analog correlator. The autocorrelation channels are for determining the rms values of density ($\tilde{n}$) and poloidal electric field fluctuations ($\tilde{E}_p$). The cross-correlation channel serves for determining the fluctuation-induced particle flux Γ.

surface. The tips are 2 mm long and 0.9 mm in diameter, and the distance between them is d = 2.5 mm. The density fluctuations δn_e were deduced from the ion saturation current on the negatively biased tip:

$$\delta n_e = \frac{2\delta I_s}{eA_p c_s} , \qquad (1)$$

where the symbol δ denotes the fluctuating part of a quantity, A_p is the probe area, $c_s = \sqrt{\frac{T_e+T_i}{M_i}}$ is the ion sound velocity (for Z = 1) and M_i the mass of ion. To obtain the absolute value of δn_e, the electron temperature should be measured independently.

The other two tips measure the floating potential, and the differential signal from them serves to determine the poloidal electric field fluctuations δE_p:

$$\delta E_p = \delta(V_{f1} - V_{f2})/d \ , \tag{2}$$

where V_{f1}, V_{f2} are the floating potentials of the tips with respect to the tokamak vessel, $V_f = U_s - \frac{kT_e}{e} \ln\left(\frac{M_i}{m_e}\right)$ for a Maxwellian plasma, and U_s is the space potential. It should be noted that only E_p fluctuations with poloidal wave numbers $k_p < 2\pi/d$ are correctly recorded.

Such an interpretation of the probe signals assumes that the fluctuations of the electron temperature are negligible [14]. However, recent experiments on TEXT [15] have shown that the relative levels of T_e and n_e fluctuations can be comparable at the plasma edge. Since T_e fluctuations were not measured during this experiment, the absolute fluctuation levels reported here should be taken as a rough estimate.

The fluctuating signals are connected to a three-channel analog correlator [16] with a flat frequency response in the range of 0.005 - 1 MHz. The arrangement of the correlator is also shown in Fig. 1. Two channels operate in the autocorrelation mode and their output signals are proportional to the mean square values of the density ($\tilde{n}_e$) and poloidal electric field ($\tilde{E}_p$) fluctuations:

$$I_{\tilde{n}} \approx \tilde{n_e}^2 = <(\delta n_e)^2>_T \ , \qquad I_{\tilde{E}} \approx \tilde{E_p}^2 = <(\delta E_p)^2>_T \ . \tag{3}$$

The third channel operates in a cross-correlation mode and its output signal is proportional to the fluctuation-induced flux Γ caused by the cross-field drift $\vec{E}_p \times \vec{B}_T$:

$$I_\Gamma \approx \Gamma = <\delta n_e \delta E_p>_T / B_T \ . \tag{4}$$

Here, the brackets $< ... >_T$ denote time averaging over an interval sufficiently long in relation to the characteristic fluctuation period ($T \doteq 0.5\ ms$ in our case).

The fluctuation data could be compared with quantities characterizing the global particle/energy confinement. With the turbulent transport assumed to be the dominant channel for anomalous particle losses, the turbulent flux $\Gamma(a)$ measured at the last closed magnetic surface can be related to the global particle confinement time τ_p as

$$\tau_p \approx a\langle n_e \rangle / \Gamma(a) \ . \tag{5}$$

Here, $\langle n_e \rangle$ is the volume averaged density. However, to allow a quantitative comparison, the turbulent flux $\Gamma(a)$ should be uniform around the torus.

In fact, the electrostatic fluctuations may also play a role in the radial energy transport. The convected energy flux due to electrostatic fluctuations $q_{conv} = \frac{5}{2} kT\Gamma(a)$ may dominate in the edge region (T is the edge temperature), as has been found on TEXT [15], but only for densities $n_e \geq 2 \cdot 10^{19}\ m^{-3}$.

3 Global confinement during LH-power scan

A link between the electrostatic fluctuations at the plasma edge and the global confinement was studied in LHCD regimes with the safety factor q(a)=3.2 (B_T = 2.8 T, $I_p = 420\ kA$) and at the line average density $\bar{n}_e = 1.3 \cdot 10^{19}\ m^{-3}$, the working gas being deuterium. It should be noted that $\bar{n}_e$ is far below the 2.45 GHz density limit on ASDEX ($\bar{n}_e^{DL} \approx 4.5 \cdot 10^{19}\ m^{-3}$) [1].

The aim of the experiment described was to determine the variation of the global and edge plasma parameters with the LH power. To avoid possible scattering of experimental data, the power scan was carried out during a single ASDEX shot (see Fig. 2 and Fig. 3). Pre-programming of the LH system allowed us to launch the lower hybrid wave in eight steps covering a broad range of powers with respect to the initial OH input ($0.025P_{OH}^o \leq P_{LH} \leq 1.3P_{OH}^o$, $P_{OH}^o \doteq 390\ kW$), see Fig. 2a. The duration of each step was chosen sufficiently long in relation to the global particle/energy confinement times.

3.1 Energy confinement

During the LHCD part of the discharge, the loop voltage and, consequently, the residual ohmic power $P_{OH} = I_p U_L^{LH}$ gradually decrease. Note also that the total power $P_{TOT} = P_{LH} + P_{OH}$ is well below the initial ohmic input during a significant part of the power scan. It reaches its minimum $P_{TOT} \doteq 0.8P_{OH}^o$ during the fourth power step (Fig. 2b).

The total energy W_{TOT} stored in the plasma is derived from magnetic measurements of the quantities β_{equ} and β_{dia}. Here $\beta_{equ} = (\beta_p^{\parallel} + \beta_p^{\perp})/2$ is the poloidal beta value, determined from equilibrium fields on the assumption that the internal inductance of the plasma remains unchanged during the LH-power scan [1]. The symbols $\parallel$ and $\perp$ denote components parallel and perpendicular to the toroidal magnetic field, respectively. $\beta_{dia} = \beta_p^{\perp}$ is the perpendicular beta determined from the diamagnetism of the plasma. The observed difference in the two betas, $\beta_{equ} > \beta_{dia}$, indicates strong anisotropy of the electron distribution, which appears to be due to the creation of suprathermal electrons during LHCD. [1] The total energy W_{TOT} is derived by means of the total beta [1], $\beta_p^{TOT} = (2\beta_{equ} + \beta_{dia})/3$.

The resulting global energy confinement time $\tau_E = W_{TOT}/P_{TOT}$ starts to increase from the beginning of the power scan, reaching its maximum $\tau_E^{max} \doteq 1.6\tau_E^{OH}$ during the fourth power step (see Fig. 2d).

However, at the same time, the YAG laser light scattering data show that the central electron temperature and density as well as their radial profiles remain close to their OH values. The central electron temperature decreases only slightly for 30 kW < P_{LH} < 100 kW ($\Delta T_e/T_e \simeq -0.15$) and the line average Z_{eff} is nearly constant; see Fig. 4. Therefore, the energy stored in the bulk electrons W_{bulk} and, consequently, the lower limit of the actual energy confinement time of the bulk electrons $\tau_E' = W_{bulk}/P_{TOT}$ remain approximately unchanged during the major part of the LH-power scan. The improvement in global confinement time

[1] The CX diagnostics shows that the energy stored in the ion component does not change.

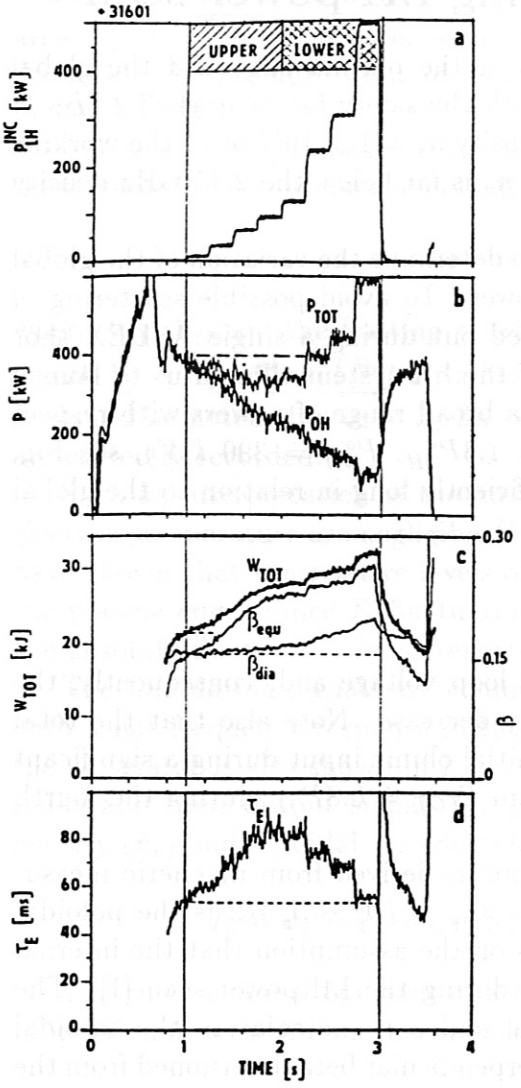

Figure 2: Evolutions characterizing the global energy balance in shot # 31601 with the LH power scan: a) incident LH power, b) residual ohmic P_{OH} and total P_{TOT} power inputs, c) poloidal betas determined from the equilibrium fields β_{equ} and diamagnetism of the plasma β_{dia} and the resulting total energy stored in the plasma W_{TOT}, d) global energy confinement time $\tau_E = W_{TOT}/P_{TOT}$.

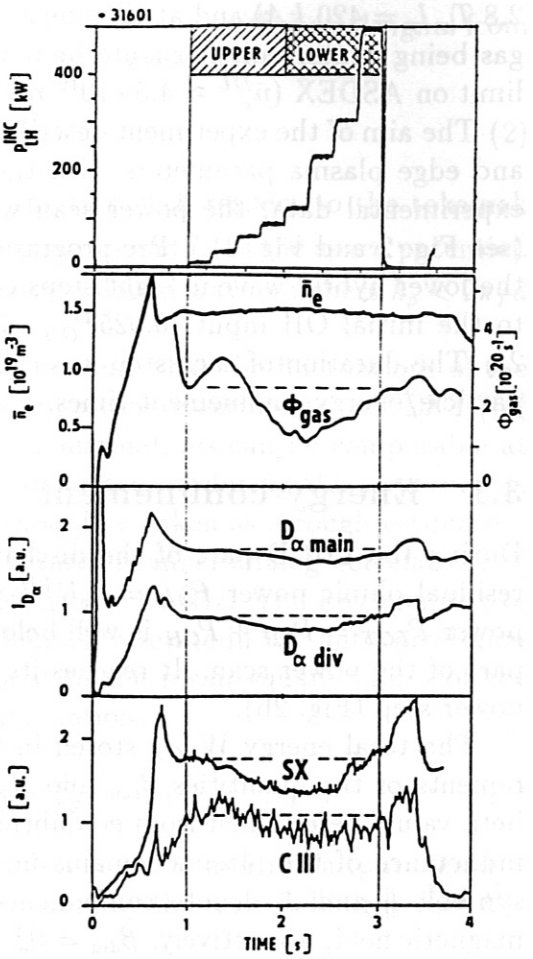

Figure 3: Evolutions characterizing the global particle confinement during the LH power scan for shot # 31601: $\bar{n}_e$ - line average density, Φ_{gas} - total influx of deuterium atoms into the plasma, $I_{D\alpha}$ - intensity of the D_α spectral line, SX - soft X-ray intensity at the central chord, CIII - intensity of the carbon line in the divertor region.

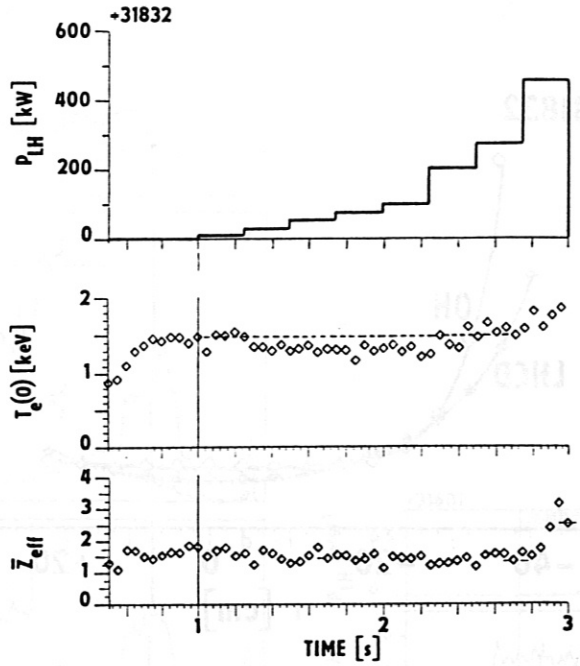

Figure 4: Evolution of the central electron temperature and the line-averaged Z_{eff} (YAG-laser data) for shot # 31832 with the LH-power scan.

has to be attributed therefore to improved confinement of the energy content of the suprathermal electron population.

3.2 Particle confinement

The behaviour of the global particle confinement during the LH-power scan was deduced from the traces shown in Fig. 3.

The plasma density is controlled by a gas valve. The total flux ϕ_{gas} of neutral atoms, which is necessary to keep the line average density around $\bar{n}_e \doteq 1.3 \cdot 10^{19}\ m^{-3}$, is reduced by a factor of two during the first half of the LH-power scan. Simultaneously, the D_α spectral line intensities from the main chamber and divertor regions decrease as well. Light and heavy impurity radiation decrease, as seen from CIII and soft X-ray radiation. Moreover, Z_{eff} drops near the plasma edge for these low LH powers; see Fig. 5. Therefore, it is concluded that the global particle confinement improves during the LH-power scan, reaching its maximum during the fourth power step, when the LH power is $P_{LH} \doteq 75\ kW$.

As in the case of the global energy confinement, all the traces depicted in Fig. 3 and, consequently, the global particle confinement time return to their initial OH values during the second half of the LH-power scan.

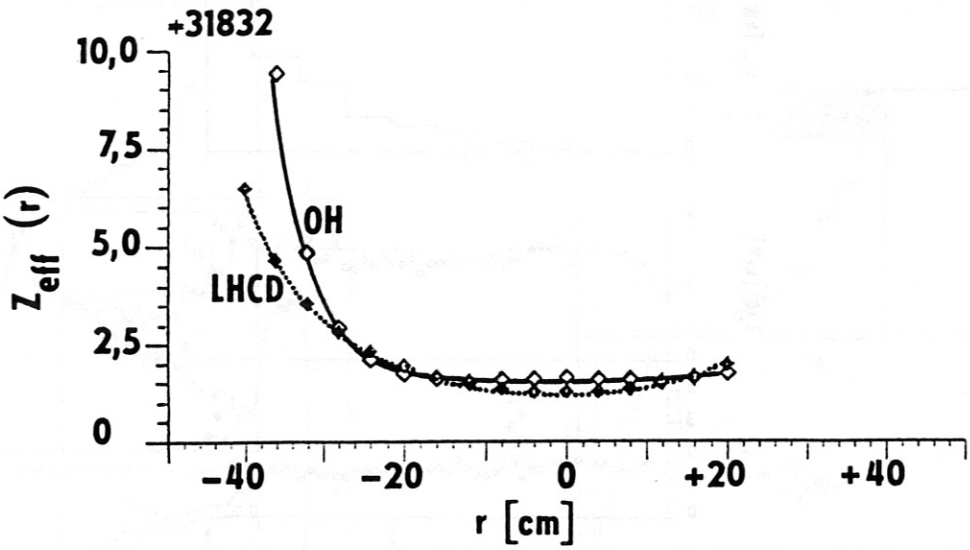

Figure 5: The radial profile of Z_{eff} during OH (t = 0.9 s) and LHCD (t = 1.5 s) phases of shot # 31832.

4 Edge fluctuations

The Langmuir probe is located 3 cm outside the separatrix (to protect the tips from damage by suprathermal electrons), within a flux tube which crosses the edge region in front of the lower grill ($R_g - R_p = 1.5\ cm$).

The evolution of the rms values of the density ($\tilde{n}$) and poloidal electric field ($\tilde{E}_p$) fluctuations are shown in Fig. 6, the corresponding steady-state values of the ion saturation current and floating potential being shown in Fig. 7. The evolutions of the density and E_p fluctuations are similar in character:

a) During the first half of the power scan, the fluctuation levels start to decrease noticeably. The maximum reduction of fluctuations is observed during the fourth power step, where the relative level of density fluctuations $\tilde{n}/n \doteq 0.22$ represents about 75 % of this OH level. The $\tilde{E}_p$ fluctuations are reduced from $\tilde{E}_p^{OH} \simeq 10V/cm$ to $\tilde{E}_p \simeq 9V/cm$.

b) On the other hand, the edge fluctuations are substantially enhanced for the last four power steps. The increase is more pronounced for the E_p fluctuations, which rise up to $\tilde{E}_p \approx 50\ V/cm$. The relative density fluctuation level reaches the value $\tilde{n}/n = 0.8$. A similar increase is also observed on the signal from the cross-correlation channel which corresponds to a significant enhancement of the fluctuation-induced flux Γ.

It should be noted that the observed increase of fluctuations occurs together with switching between the two LH antennae from the upper to the lower grill.

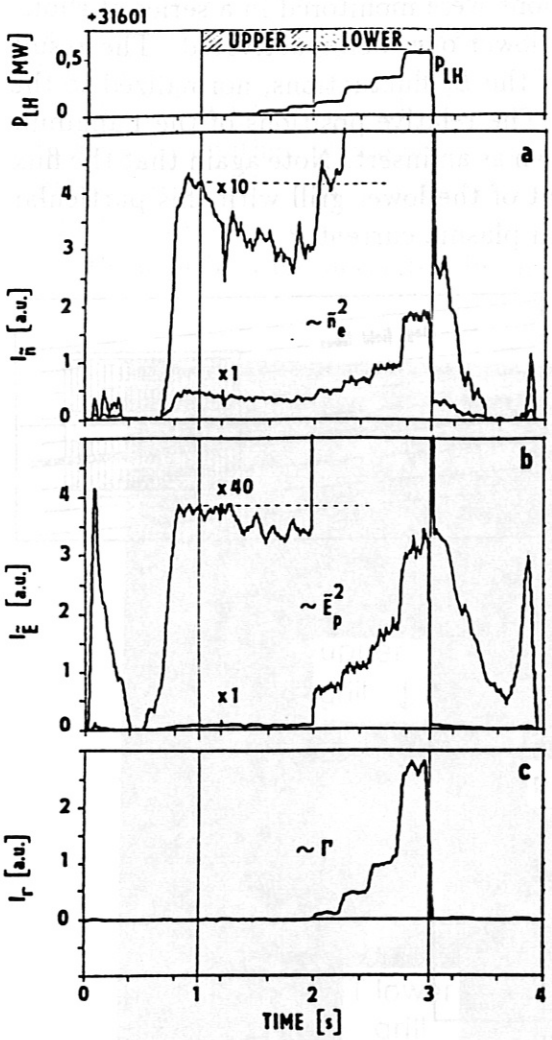

Figure 6: Evolution of the rms values of the electrostatic fluctuations during shot # 31601 with the LH power scan. The sequence of the grill activation is indicated at the top:
a) density fluctuations $\tilde{n}$,
b) poloidal electric field fluctuations $\tilde{E}_p$,
c) fluctuation-induced particle flux Γ.

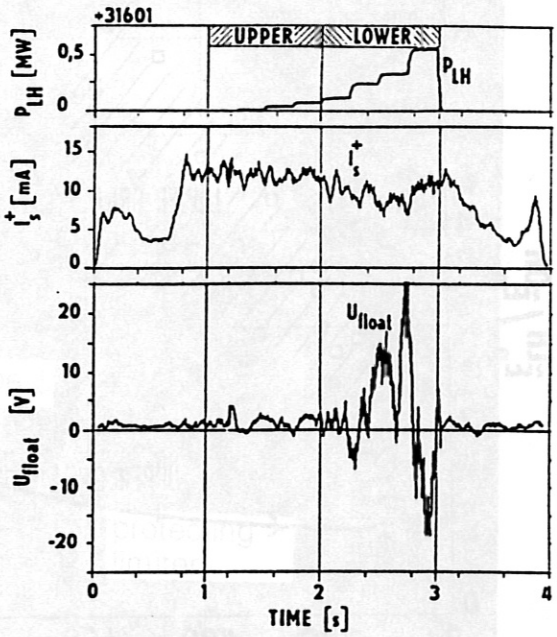

Figure 7: Steady-state values of the ion saturation current and floating potential during the LH power scan (# 31601).

This suggests that the relative positions of the probe and the active grill might be important for a correct interpretation of the fluctuation data.

In order to clarify this, the edge fluctuations were monitored in a series of shots, with only a single grill, either the upper or lower one, being activated. The result is depicted in Fig. 8, where the rms values of the E_p fluctuations, normalized to the OH level, are plotted versus the LH power. The relative positions of the Langmuir probe and the antenna structure are also shown as an insert. Note again that the flux tube of the probe crosses the plasma in front of the lower grill with this particular orientation of the toroidal magnetic field and plasma current.

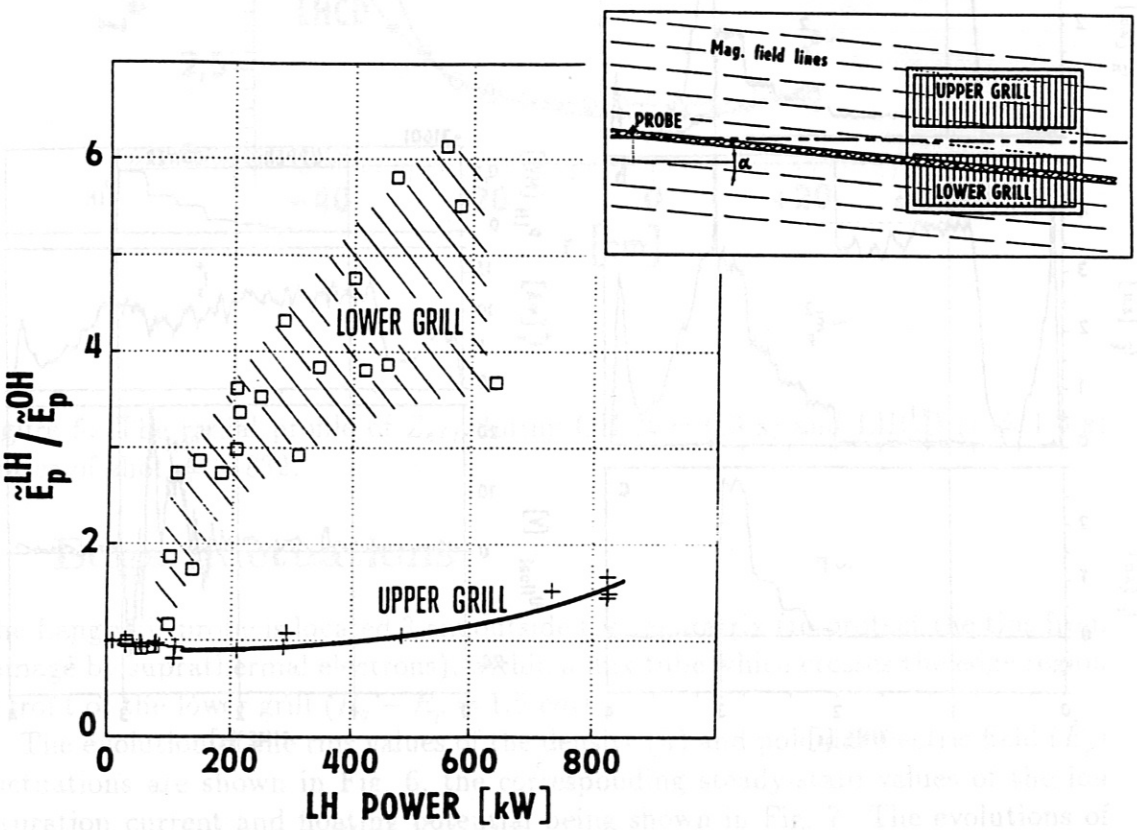

Figure 8: A plot of the normalized level of the E_p fluctuations versus LH power. The relative positions of the Langmuir probe and LH antenna structure are shown in scale as an insert. The distance between the probe and the centre of the grill along the flux tube is about 80 cm.

One can clearly distinguish three LH-power regions, each with characteristic behaviour of the fluctuations: At low powers ($P_{LH} < 100\ kW$) the fluctuations are reduced independently of the fact whether the lower or upper grill is activated. At medium powers, the fluctuations increase only if the active grill is connected by a flux tube with the probe. In the other case, a reduction of fluctuations is observed as with low powers. At still higher powers ($P_{LH} > 400\ kW$), the fluctuations increase above the OH level in both cases. Nevertheless, a more pronounced enhancement of fluctuations is observed if the active grill is connected to the probe.

We suggest the following interpretation of the data in Fig. 8: For LH powers higher than a threshold value ($P_{LH} > 100\ kW$ in this particular case), a region with

enhanced turbulence is created in front of the active grill and extends in the toroidal direction along the magnetic field lines. Its toroidal length is at least comparable with the probe-grill distance ($\sim$ 80 cm) and its width in the poloidal direction seems to be comparable (at least for medium powers $P_{LH} < P^{o}_{OH}$) to the height of the grill.

We believe that the observed enhancement of the edge fluctuations could be related to another phenomenon, resulting from a local modification of the edge plasma at LHCD. This can be seen immediately from a photo taken during LHCD which shows a toroidal view of part of the interior of the ASDEX vessel; see Fig. 9. Both grills were activated in this particular case. The photo shows a bright

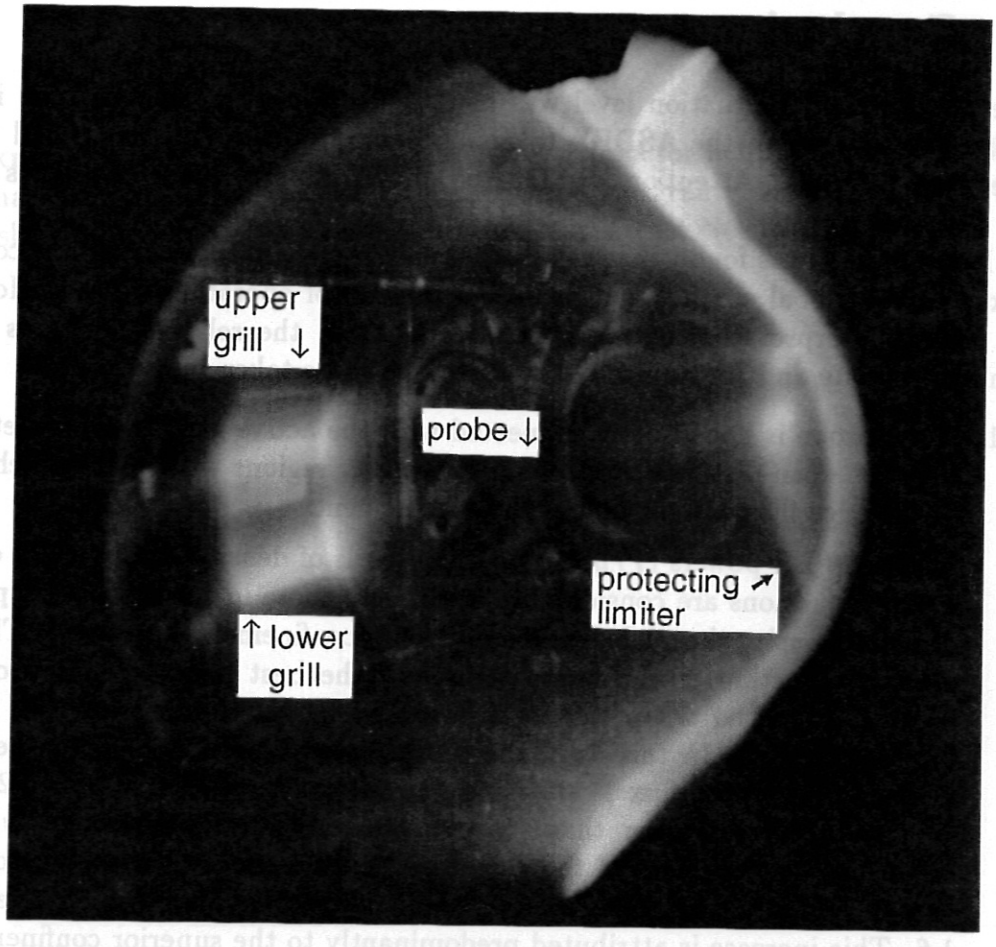

Figure 9: A photo showing bright bands in front of the grills, which are both in operation. Note that the bands spread toroidally along the magnetic field lines and produce light patterns on the protecting limiter.

zone in front of the two grills . In addition to the bright regions just in front of the grills, there is some enhanced light emission from bands extending toroidally away from the grills. Their poloidal pitch corresponds to a helix with the rotational transform $1/q(a)$. It should be noted that this phenomenon was seen in all cases during LH wave injection activated with all wave spectra applied. This effect has

been attributed to local power deposition in front of the grill due to nonlinear effects [17].

As indicated in the photo, the position of the probe is inside the bright band connected with the lower grill. Therefore, the parameters measured with the probe during activation of this grill should be strongly influenced by local nonlinear processes. This is also apparent for the probe steady-state data shown in Fig. 7 . The ion saturation current is slightly lower then the initial OH value and, in particular, a considerable variation of the floating potential is observed in this case. The latter may reflect some changes of the space potential in front of the active grill, already reported in [18].

5 Conclusions

The electrostatic fluctuation level was measured during LH current drive in low-density discharges on the ASDEX tokamak and compared with the global particle/energy balances. Attention was focused on variation of these quantities versus the LH power.

In general, it was found that the level of edge electrostatic fluctuations could be linked to the global confinement in LHCD regimes of operation as well. However, for correct interpretation of the experimental data, the relative positions of the Langmuir probe and LH antenna structure have to be taken into account:

1. If the probe is not directly connected with the active grill by a magnetic flux tube, one can distinguish the following power regions with specific behaviour of the edge fluctuations and global confinement:

   i) For low LH powers ($P_{LH} < P^o_{OH}$), the levels of density and poloidal electric field fluctuations are considerably lower than those in the OH target plasma. Simultaneously, the global particle/energy confinement improves. The maximum reduction of the fluctuations and the best particle/energy confinement are reached when the total power input has a minimum (at $P_{LH} = 0.2 - 0.25 P^o_{OH}$). In this case, the product $\tilde{n}.\tilde{E}_p$ (proportional to the radial fluctuation-induced flux Γ via a crosscorrelation coefficient $c_{nE} = 0.2 - 0.5$) is a factor of 1.5 lower than its OH value . This is consistent with the estimated improvement of the global particle confinement time (up to factor of 2). Similarly, the global energy confinement time increases by a factor of 1.6. This increase is attributed predominantly to the superior confinement of suprathermal electrons. Although the quantity W_{bulk}/P_{TOT} remains close to the ohmic level, the energy confinement time of the bulk electrons defined as $\tau_E^{bulk} = W_{bulk}/P_d$ seems to increase, since the actual power deposited in the bulk electrons P_d is only a fraction of the total power input P_{TOT} (e.g. due to the direct power loss caused by radial transport of the suprathermal electrons).

   ii) For higher LH powers ($P_{LH} > P^o_{OH}$), enhancement of the fluctuations is observed together with deterioration of the global confinement.

2. If the Langmuir probe is connected with the active grill by a magnetic flux tube, significantly enhanced fluctuations are monitored by the probe, but only

if the LH power is above a threshold value ($P_{LH} > 100\ kW$). This suggests the creation of a turbulent region localized in a magnetic flux tube crossing the mouth of the active waveguide grill. It seems to be caused by local power deposition in front of the grill antenna.

It should be noted that the global particle/energy confinement times gradually decrease from their maximum to their initial OH values when the levels of the fluctuations inside the turbulent region increase.

Therefore, the relative positions of the probe and grill are important at high LH powers, while they are not critical at low powers, since the fluctuations are reduced for both grill-probe configurations.

Acknowledgement: The authors thank R. Klíma for helpful discussions. The final phase of this work was partially supported by grant No. 14310 from the Czechoslovak Academy of Sciences and by IAEA contract No. 6702/RB.

References

[1] Söldner F. et al: 13th Int. Conf. on Plasma Phys. and Contr. Nucl. Fus. Res., Washington 1990, IAEA-CN-52/E-1-1

[2] Takase Y. et al: Nuclear Fusion 27, 1987, p.53

[3] Stevens J.E et al: 12th Eur. Conf. on Contr. Fusion and Plasma Phys., Budapest 1985, Vol.II, p.192

[4] Parlange F. et al: 12th Eur. Conf. on Contr. Fusion and Plasma Phys., Budapest 1985, Vol.II, p.172

[5] Alikaev V.V et al: Fizika Plazmy 11, 1985, p.53

[6] Luckhardt S.C. et al: Phys. Fluids 29(6), 1986, p.1985

[7] Nakamura M. et al: Nuclear Fusion 31, 1991, p.1485

[8] Ritz C.P. et al: Nuclear Fusion 27, 1987, p.1125

[9] Stöckel J. et al: Plasma Fusion and Controlled Nuclear Fusion Research 1988, Vol.1, p.359

[10] Stöckel J. et al: Plasma Fusion and Controlled Nuclear Fusion Research 1990, Vol.1, p.491

[11] Žáček F. et al: In Proc of 18th Eur. Conf. on Contr. Fusion and Plasma Phys., Berlin 1991, Vol.III, p.341

[12] Vayakis G.: Report AEA FUS 123, Culham Lab., April 1991

[13] Leuterer F., Söldner F., Münich M., Monaco F., Zouhar M., Bartiromo R., Tuccillo A., Bernabei S., Forest C.: Plasma Physics and Controlled Fusion, Vol.33, 1991, No.3, p.169

[14] Howling A.A., Robinson D.S.: Plasma Physics and Controlled Fusion, 30, 1988, p.1863

[15] Ritz C.P. et al: Phys. Rev. Lett., 62, 1989, p.1844

[16] Stöckel J. at al: In Proc. of 15th Czech. Seminar on Plasma Physics and Technology, Liblice, 1989

[17] Petržílka V., Leuterer F., Söldner F., Giannone L., Schubert R.: Nuclear Fusion 31, 1991,p.1758; Schubert H.: submitted to Nuclear Fusion

[18] Lenoci M., Haas G.: Rep.III/113 IPP Garching, July 1986